



OPEN

CONFERENCE  
PROCEEDINGSAPEnergy2014  
.....

SUBJECT AREAS:

FUEL CELLS

POLLUTION REMEDIATION

Received  
12 February 2014Accepted  
2 June 2014Published  
29 August 2014Correspondence and  
requests for materials  
should be addressed to  
C.-M.H.  
(hungcm1031@gmail.  
com)

# Platinum particles supported on mesoporous carbons: fabrication and electrocatalytic performance in methanol-tolerant oxygen-reduction reactions

Cheng-Di Dong, Chiu-Wen Chen, Chih-Feng Chen &amp; Chang-Mao Hung

Department of Marine Environmental Engineering, National Kaohsiung Marine University, 142 Haijhuang Road, Nanzih District, Kaohsiung City 81157, Taiwan.

In this report, we describe the preparation and electrochemical characterization of a Pt electrocatalyst, which was synthesized from hexachloroplatinic acid, using the incipient wetness impregnation method. This carbon mesoporous materials (Pt-CMMs) electrocatalyst was used for catalyzing the oxidation of methanol and its oxygen-reduction reaction. The electrocatalytic oxidation of methanol was studied using linear-sweep voltammograms (LSV), polarization and chronoamperometric measurements. Phase characterizations and morphological analyses were performed using 3D excitation-emission fluorescent matrix (EEFM) spectroscopy, UV-Vis absorption measurements, and X-ray diffraction (XRD) and environmental scanning electron microscopy (ESEM) techniques; the ESEM system was equipped with an energy-dispersive spectrometer (EDS). The oxidation capacity measured using a LSV might explain the high activity exhibited by the Pt-CMM electrocatalysts in methanol-tolerant oxygen reduction, and the results demonstrated that the potential and current density of the main reaction peak of the Pt-CMMs electrocatalyst changed during the reaction. Moreover, EEFM spectroscopy and XRD were determined to be appropriate and effective methods for characterizing Pt clusters that enhance their intrinsic emission from Pt-CMMs electrocatalysts in electrocatalytic-treatment systems. Furthermore, the ESEM-EDS results showed that fresh Pt nanoparticles were highly dispersed on CMMs and featured a 20 nm diameter and a narrow particle-size distribution.

Methanol ( $\text{CH}_3\text{OH}$ ) has attracted increasing attention worldwide because of its high energy-conversion efficiency and low-pollution emissions<sup>1-3</sup>. The energy-conversion process used in direct methanol fuel cells has attracted considerable attentions as a possible method of generating energy. To increase the electrocatalytic oxidation of methanol, substantial effort has been devoted toward developing high-performance catalysts that can potentially shorten the reaction time of the oxidation process and allow the reaction to proceed under mild operating conditions inside fuel cells. Currently, catalytic oxidation of methanol by using dedicated electrocatalysts is considered to be a suitable approach for increasing the effectiveness of advanced oxidation technology because, in this approach, various industrial electrocatalytic processes are used to potentially reduce the oxidation-reaction time and allows the oxidation to proceed under mild operating conditions<sup>4,5</sup>. From an energetic and ecological viewpoint, the electrocatalytic oxidation of methanol ( $\text{CH}_3\text{OH}$ -ECO) into a stream of  $\text{H}_2$  is considered intriguing because this reaction has been shown to be suitable for developing high-performance proton-exchange membranes and electrocatalyst materials and related membrane-electrode assemblies (MEAs)<sup>6-10</sup>. Furthermore, methanol acts as a clean  $\text{H}_2$ -energy carrier that can be used in fuel-cell applications, which is an additional benefit regarding environmental protection. Moreover, metallic catalysts are often used in this reaction because they are highly active and exhibit selectivity toward  $\text{H}_2$ .

Comparing catalysts of distinct types has shown that metallic catalysts are the most active catalysts in the oxidation reaction. Oxidation of adsorbed CO is regarded as the rate-determining step, and Pt is widely accepted to promote CO oxidation. However, when Pt is used as the catalyst, it is poisoned by the adsorption of the CO



produced during the methanol oxidation reaction (MOR). Previous, Feng et al.<sup>11</sup> examined the reaction kinetics of methanol oxidation and compared the catalytic activities reported in the literature; the results showed that PAN/PSF-based PtRu catalyst materials were used in a broad range of applications for the purpose of accelerating the electrocatalytic oxidation of methanol in its liquid phase, which contributed to improved or promising results. The oxygen-reduction reaction (ORR) is one of the most critical multistep electrochemical reactions because it is widely used in fuel cells. Platinum-based materials have been used to solve problems related to the MOR, and these materials are recognized to be the most active electrocatalysts of the ORR. Liu et al.<sup>12</sup> obtained a highly efficient and resistant ORR of methanol to H<sub>2</sub> by using a Pt-Co bimetallic catalyst supported on ordered mesoporous carbons. Moreover, Nikonova et al.<sup>13</sup>, who developed a rhenium-based oxide for catalyzing methanol oxidation, determined that the activity of fresh rhenium catalysts increases when the temperature is increased during the decomposition of methanol and that the nature of the ReO<sub>x</sub>/TiO<sub>2</sub> precursor generated during the catalysis of methanol oxidation at the catalyst surface is a critical factor involved in the selective oxidation of methanol. Huang et al.<sup>14</sup> investigated methanol decomposition to H<sub>2</sub> in a fixed-bed continuous-flow quartz reactor at 393 K and GHSV = 46000 h<sup>-1</sup>; the results demonstrated that methanol conversion reached 95% on a copper-zinc-supported gold catalyst. Furthermore, Liu et al.<sup>15</sup> developed a direct methanol fuel cell (DMFC) composed of a PtRu-carbon mesoporous material and determined that the DMFC increased the methanol-oxidizing activity and the selectivity of the catalyst. Recently, Lee<sup>16</sup> examined the electrocatalytic oxidation of methanol in a liquid stream by using an effective Pt/TiO<sub>2</sub> catalyst; a synergistic effect was detected, and the methanol-reduction activity obtained was the highest ever reported because the nitride support structure exhibited high catalytic ability and chemical stability.

Noble transition metals such as platinum-group metals, particularly Pt, have recently attracted growing research interest because they are used as three-way catalysts and electrocatalysts in fuel cells, and because they are the most active components in MORs because of their selective catalytic and oxidation-reduction potential properties<sup>17-19</sup>. The use of various functional materials has shown that these additives are also active in methanol electro-oxidation reactions<sup>20,21</sup>. For instance, the use of platinum-based metals enhances the methanol-conversion properties of electrocatalysts and increase their CO tolerance<sup>22,23</sup>.

Studying mediated electrochemical-oxidation properties is critical because these are factors that influence a catalyst's surface area, crystallite size distribution, electronic conductivity, structural stability, and catalytic properties. A previous study<sup>24</sup> demonstrated that precious metal (Pt) catalysts exhibit high catalytic activities and they can be used for elucidating the reduction characteristics of the methanol conversion that occurs in a catalytic oxidation and dehydrogenation system. Moreover, the interaction between platinum oxide and CMMs is complex: various metal interactions can produce synergistic effects that enhance their catalytic characteristics<sup>25</sup>. Conversely, the use of a platinum-based catalyst is recognized as an alternative approach for enhancing electrocatalytic performance in certain reactions<sup>26,27</sup>. However, few studies have used a Pt-composite CMMs (Pt-CMMs) substrate to determine the reactive characteristics of these active metals during electrocatalytic liquid-phase oxidation of methanol.

Currently, linear-sweep voltammogram (LSV) measurements are widely used for evaluating the electrochemical activity of a catalyst. In the case of most catalysts, the excitation-emission fluorescence matrix (EEFM) spectroscopy data on their fluorescence emissions are available because the catalysts have been chemically and physically characterized in detail. However, although these fluorescence emissions have been studied for decades, particularly in the case of platinum-based composite materials, little information has been

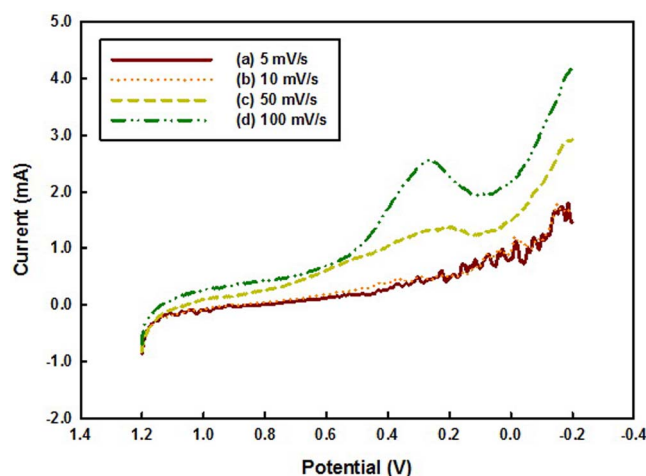


**Figure 1** | Linear sweep voltammogram profiles in a 0.5 M H<sub>2</sub>SO<sub>4</sub> electrolyte solution recorded at various scan rates for the Pt-CMMs electrocatalyst.

obtained regarding the fluorescence effects of most newly developed materials and their interactions with metal structures. In this study, we used EEFM spectroscopy across a range of excitation and emission wavelengths as a method to effectively examine the characteristics of catalysts during the catalytic process. Thus, we investigated the application of an electrocatalytic oxidation technique in which the activity of Pt-CMMs was studied during the MOR occurring within an acidic medium under various conditions by using LSV measurement of the ORR processes. The catalyst used was also characterized by analyzing data obtained using polarization, chronoamperometric, UV-Vis, and EEFM spectroscopy, X-ray diffraction (XRD) analysis, and environmental scanning electron microscopy (ESEM) performed using a system equipped with an energy-dispersive spectrometer (ESEM-EDS).

## Results

**Effect of various scan rates on the oxygen-reduction reaction conducted using Pt-CMMs electrocatalysts: reaction in a sulfuric-acid solution.** The experiments were conducted in a 0.5 M H<sub>2</sub>SO<sub>4</sub> medium and LSV curves were obtained at various scan rates ranging from 5 to 100 mV/s. In this medium, the complex Pt-CMMs electrocatalyst displayed little reactivity in the potential

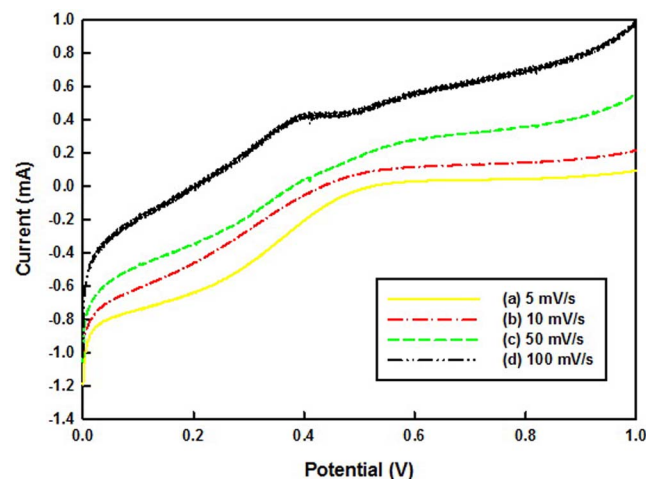


**Figure 2** | Polarization curves for ORR on the Pt-CMMs electrocatalyst in O<sub>2</sub> saturated 0.5 M H<sub>2</sub>SO<sub>4</sub> solution at various scan rates and a rotating speed of 1600 rpm.

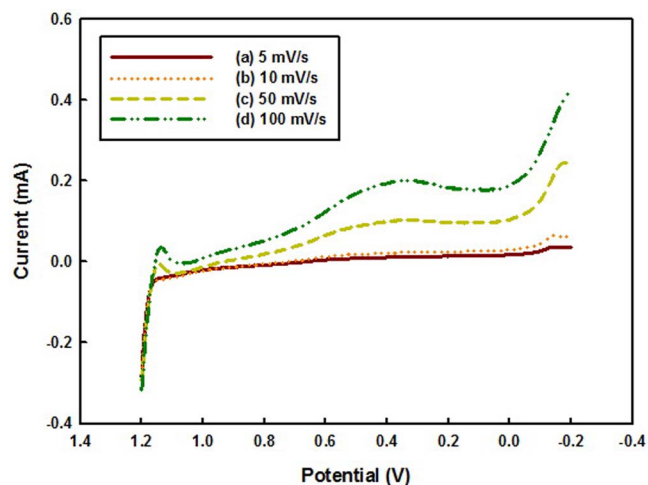


**Figure 3** | Linear sweep voltammogram profiles in  $O_2$  saturated 0.5 M  $H_2SO_4$  + 0.5 M  $CH_3OH$  solution electrocatalytically recorded at various scan rates for the Pt-CMMs electrocatalyst.

window when the scan rate was either 5 or 10 mV/s (Fig. 1). The LSV curves revealed that the Pt-CMMs electrocatalyst exhibited elevated redox capacities when the potential scan rates were increased (from 50 to 100 mV/s): notable oxidation peaks at 0.3 and 0.25 V and respective increased currents were observed (Fig. 1). Proton adsorption on Pt surfaces was observed at potentials under 0.3 V, and this was followed by the hydrogen-evolution reaction<sup>28</sup>. We also conducted experiments in which polarization profiles and onset potentials were used for the ORR at various scan rates ranging from 5 to 100 mV/s; the reaction was in a 0.5 M  $H_2SO_4$  medium and the reaction mixture was rotated at 1600 rpm at room temperature. The results showed that the current increased linearly when the scan rates were increased. In 0.5 M  $H_2SO_4$ , complex Pt-CMM electrocatalyst displayed little reactivity in the potential window when the scan rate was either 5 or 10 mV/s (Fig. 2). A previous study suggested that at low potential scan rates, the electrode reaction was controlled by adsorption, whereas at high potential scan rates, the reaction was diffusion controlled<sup>29</sup>. The LSV curves further revealed that the Pt-CMMs electrocatalyst exhibited elevated redox capacities when a higher potential scan rates was used (100 mV/s): a notable onset potential at 0.4 V and its respective increased currents were observed (Fig. 2).

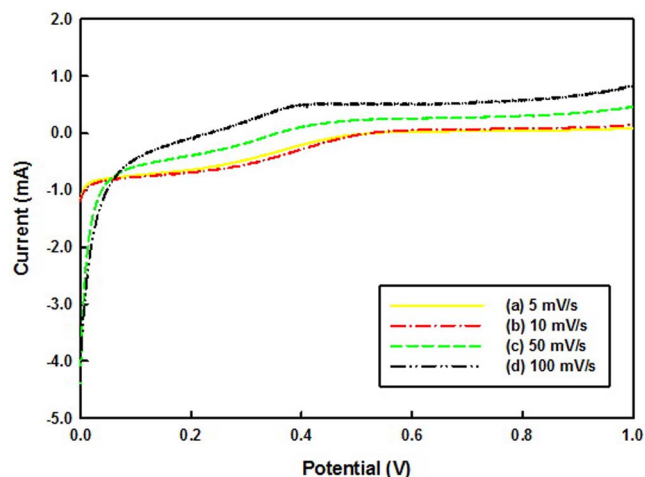


**Figure 4** | Polarization curves for ORR on the Pt-CMMs electrocatalyst in  $O_2$  saturated 0.5 M  $H_2SO_4$  + 0.5 M  $CH_3OH$  solution at various scan rates and a rotating speed of 1600 rpm.

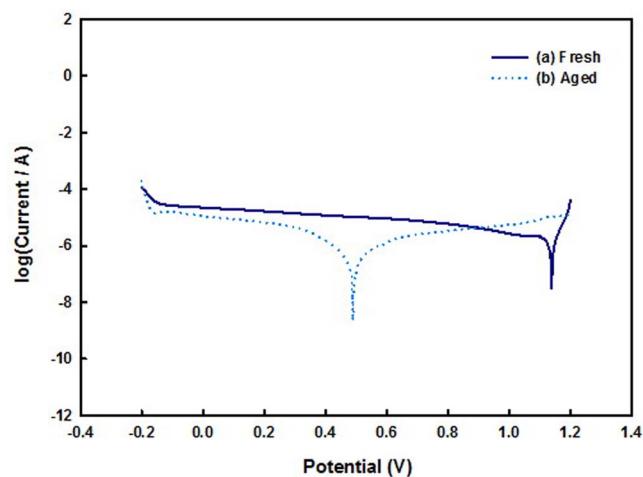


**Figure 5** | Polarization curves of the Pt-CMMs electrocatalyst in  $O_2$  saturated 0.5 M  $H_2SO_4$  + 0.5 M  $CH_3OH$  solution (a) before and (b) after the electrocatalytic test.

**Effect of various scan rates on the oxygen-reduction reaction conducted using Pt-CMMs electrocatalysts: reaction in a methanol solution.** To investigate the properties of the complex Pt-CMMs electrocatalyst, we conducted the following experiments, in which LSV scan rates were used that ranged from 5 to 100 mV/s, and a 0.5 M methanol-oxidation reaction was performed with in a 0.5 M  $H_2SO_4$  medium (Fig. 3). A rapid rise in current density was not detected until a potential of approximately 0.6 V, and this rise was observed when a scan rate of 100 mV/s was used (Fig. 3). Thus, increasing the scan rates increased the range of the current. Furthermore, the LSV plots revealed that the Pt-CMMs electrocatalyst exhibited an elevated oxidation current density when a wide peak of current density was reached in the MOR at approximately 0.4 V and 0.2 mA. This oxidation capacity suggested that the catalyst exhibited substantial activity in methanol-tolerant oxygen reduction because the number of electrochemically active sites that are formed was increased. Moreover, a potential peak was generated at 0.6 V during the forward scan because of the catalytic activity that occurs during methanol oxidation, and an onset potential was observed near 0.2 to 0.4 V during the reverse scan and this represents the effectiveness of the removal of the incompletely oxidized carbonaceous species that are formed during the oxidation reaction<sup>4,15</sup>. A previous study demonstrated that CMM

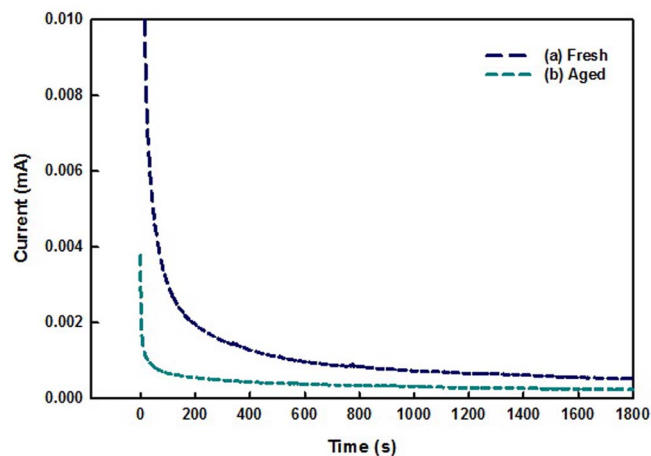


**Figure 6** | Chronamperometric measurements of the Pt-CMMs electrocatalyst in  $O_2$  saturated 0.5 M  $H_2SO_4$  + 0.5 M  $CH_3OH$  solution (a) before and (b) after the electrocatalytic test.

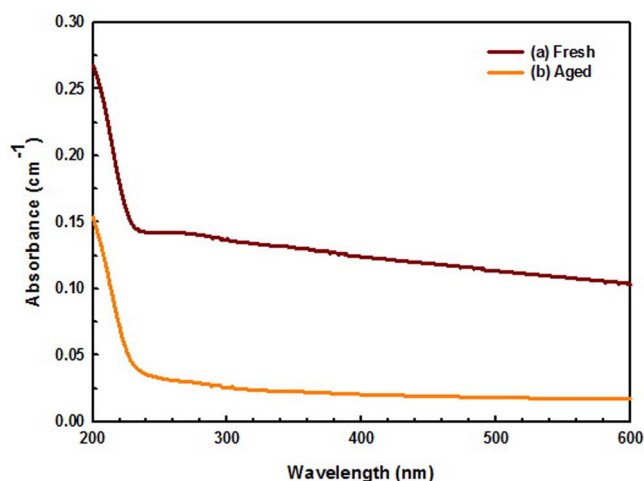


**Figure 7** | UV-Vis absorption spectra of the Pt-CMMs electrocatalyst (a) before and (b) after the electrocatalytic test.

can function as a substrate because residual oxygen-containing functional groups are generated in the catalytic reaction and the CMMs strongly promote oxygen storage on the catalyst surface<sup>26</sup>. To further evaluate the electrocatalytic activities of the complex

Pt-CMMs electrocatalyst, we conducted experiments in which polarization profiles and onset potentials were used for the ORR at scan rates ranging from 5 to 100 mV/s; a 0.5 M methanol oxidation reaction was performed within a 0.5 M H<sub>2</sub>SO<sub>4</sub> medium (Fig. 4). A rapid rise in current density was not detected until an onset potential of 0.42 V, and this rise was observed when a scan rate of 100 mV/s was used (Fig. 4); this indicated the occurrence of the MOR. Thus, increasing the scan rates increased the range of the current. Furthermore, the polarization plots revealed that the Pt-CMMs electrocatalyst exhibited an elevated oxidation current density when a wide peak of current density was reached in the MOR at approximately 0.42 V. This catalytic performance in the electrooxidation of methanol suggests that the catalysts exhibited high activity in methanol-tolerant oxygen reduction because the numbers of electrochemically active sites and porous structures that were formed were increased. At scan rates of 5 and 10 mV/s, the complex Pt-CMMs electrocatalysts generated diminished methanol-oxidation peak currents in a given potential window (Fig. 4). Oliveira<sup>19</sup> demonstrated that the adsorption and desorption of oxygen-containing PtOH species play key roles in methanol catalytic electrolysis and hydrogen evolution. Moreover, certain incompletely oxidized carbonaceous intermediates of this reaction are adsorbed at the surface of electrode, which might lead to a loss of electrocatalytic activity.

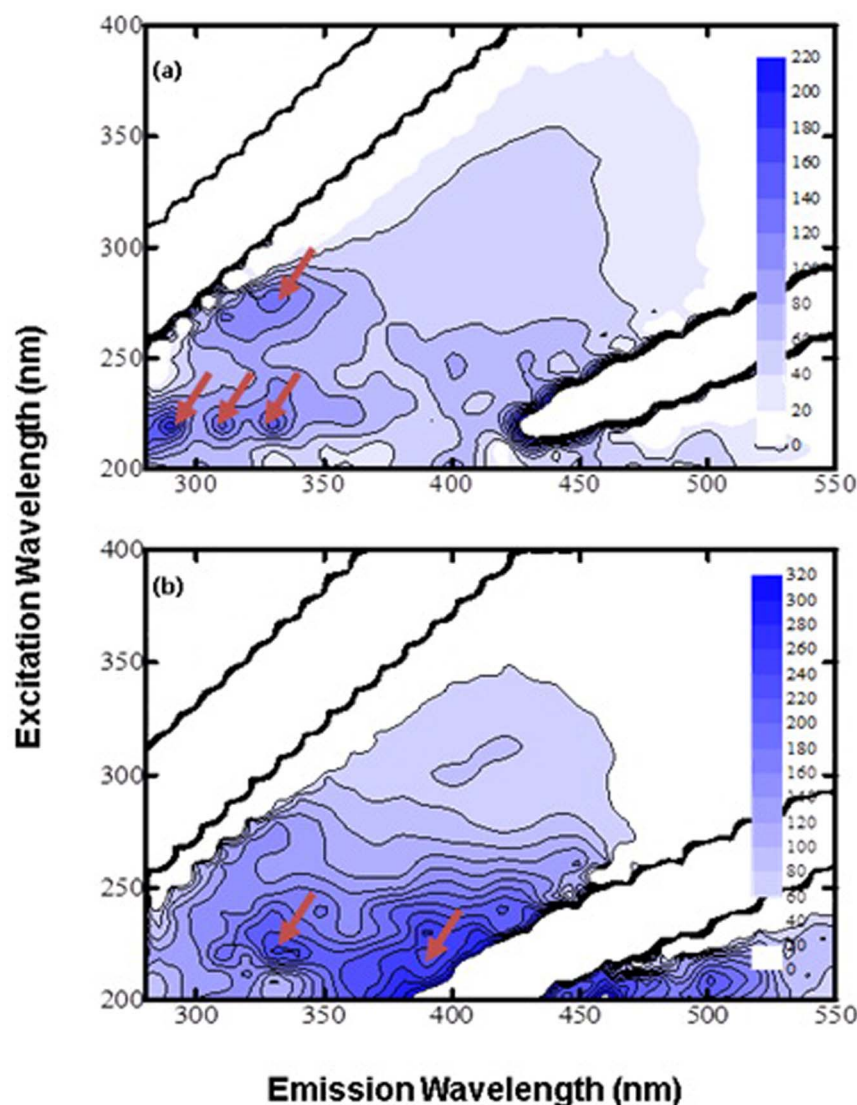


**Figure 8** | Contour plots of the excitation-emission fluorescent matrix for the Pt-CMMs electrocatalyst (a) before and (b) after the electrocatalytic test.

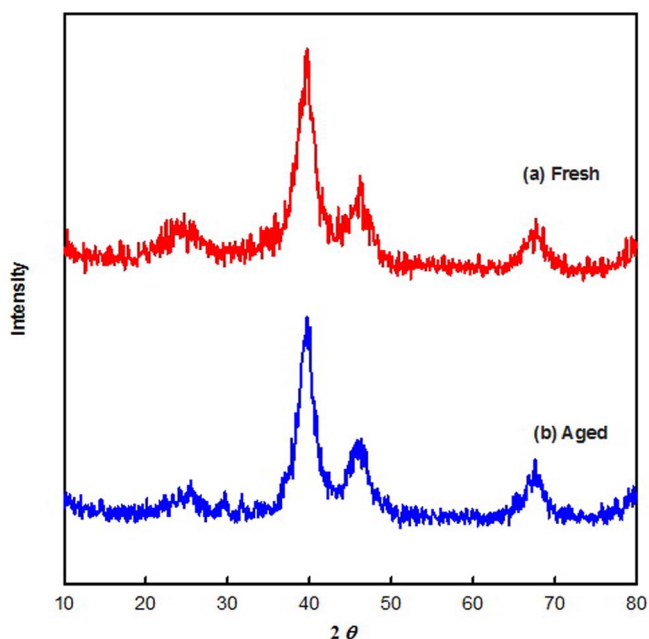


**Figure 9** | XRD of the Pt-CMMs electrocatalyst in a 0.5 M H<sub>2</sub>SO<sub>4</sub> + 0.1 M CH<sub>3</sub>OH solution (a) before and (b) after the electrocatalytic test.

**Pt-CMMs electrocatalyst performance.** To elucidate the corrosion properties of the complex Pt-CMMs electrocatalyst, we conducted experiments in 0.5 M H<sub>2</sub>SO<sub>4</sub> by using the polarization curve profiles, and we performed the MOR in an acidic medium by using the equilibrium potential ( $V_{eq}$ ) (Fig. 5). In 0.5 M H<sub>2</sub>SO<sub>4</sub>, the Pt-CMM electrocatalyst generated a shoulder peak at approximately 1.18 V in the potential window, which is shown as the equilibrium potential  $V_{eq}$  (Fig. 5a). Moreover, the polarization-curve plots revealed that in 0.5 M methanol, the Pt-CMMs electrocatalyst generated a notable potential peak at 0.5 V, which is far from the corrosion potential of the catalyst (Fig. 5b). Furthermore, we conducted experiments in 0.5 M H<sub>2</sub>SO<sub>4</sub> by using the chronoamperometric-curve profiles, and we performed the MOR in an acidic medium at 0.5 V (Fig. 6). The Pt-CMMs electrocatalyst exhibited higher current densities in 0.5 M methanol compared with the densities generated by aged samples (Fig. 6b), and the currents gradually stabilize over time and attained a steady state. This oxidation capacity suggests that the initial high current corresponds mainly to double-layer charging and that the electrocatalyst is highly resistant to poisoning in the MOR. Moreover, the results showed that the oxidation current measured in the aged sample decreased rapidly because of irreversible CO poisoning<sup>19</sup>.

To delineate the electrochemical properties of the complex Pt-CMMs electrocatalyst, we measured UV-Vis absorption spectra (Figure 7), which provided information on the states of the platinum species in the catalyst. The results revealed that bands associated with an octahedral platinum (IV) species were observed at 228 nm<sup>30</sup> (Fig. 7a) and that the UV-Vis absorption spectra displayed only minor changes (Fig. 7b). Notably, the active metal, complex Pt, and the CMMs typically exhibited strong synergistic relationships when they were prepared as a complex Pt-CMMs substrate catalyst<sup>31</sup>.

To further characterize the reactive properties of the catalyst, we analyzed the excitation/emission plot positions generated from the data obtained by performing EEFM spectroscopy. Figure 8a displays 3D-EEFM fingerprint obtained for fresh complex Pt-CMMs; four noteworthy excitation/emission plots were generated at 220/250, 220/320, 220/330 and 275/340 nm. Figure 8b displays the EEFM fingerprint of the Pt-CMMs catalyst that was obtained after the activity test; in this case, two notable excitation/emission plots at 220/340 nm and 220/400 nm were observed instead of four plots.

Figure 9 displays the XRD patterns of the fresh and used catalysts, which reveal that the catalyst changed during exposure to the electrocatalytic environment. Furthermore, the XRD analysis confirmed the existence of the PtO<sub>2</sub>/Pt<sup>0</sup> states of the Pt-CMMs catalyst. The dominant PtO<sub>2</sub> diffraction peaks of the Pt-CMMs catalyst were detected at  $2\theta$  values of approximately 42.5°<sup>32</sup>. The dominant (200) and (220) planes of the face center cubic (fcc) structure of the Pt<sup>0</sup> diffraction peak of this catalyst were detected at  $2\theta$  values of approximately 47.5° and 67.4°, respectively. This result agrees with the data that Shin<sup>33</sup> obtained for this system. Moreover, the two peaks at  $2\theta$  values of approximately 25.9° and 43.2° are the (002) and (101) diffraction planes of the amorphous and hexagonal carbon support, respectively<sup>34</sup>.

To characterize the surface of the fresh and aged catalyst, we examined the changes in the surface morphology of the catalyst by using SEM-EDS (Fig. 10). The EDS provided evidences of the presence of Pt and carbon in the composite. The ESEM results showed that the Pt nanoparticles were highly dispersed on the CMM and featured a diameter of 20 nm and a narrow particle-size distribution (Fig. 10). Furthermore, the surface of the catalyst appears more aggregated and crystalline in Fig. 10a than in Fig. 10b; the result presented in Fig. 10b indicates that disaggregated and dispersed phases were formed when the surface of the catalyst was aged or when it was poisoned because of plugging or carbon corrosion, which implies that the porosity of the particles had changed. These crystal phases might account for the high activity of the catalysts. These results also confirm that the dispersion phenomena exhibited by the catalyst increased the efficiency of methanol oxidation.

## Discussion

In this study, we determined that current density increased when the potential scan rate was increased; this can be attributed to the excitation signal generated during the charging of the interface capacitance by the charge-transfer process<sup>35</sup> (Fig. 1 and 2). In a previous study, the current-density peak in this type of an electrochemical reaction was demonstrated to be approximately 0.25 V, because the reaction involves a strong adsorption of hydrogen<sup>36</sup>. Furthermore, the generation of a platinum hydroxide species (Pt(OH)<sub>x</sub>) has been shown to generate reduction peaks at 0.5 V<sup>37</sup>. However, when this CMM is in the presence of a platinum catalyst, the adsorption can be assumed to promote the formation of the electrocatalytically active phase of PtO<sup>12</sup>.

When present with a platinum catalyst, the CMM can also be assumed to promote the formation of the active phase of PtO during methanol oxidation<sup>27</sup>. Moreover, the overall methanol electro-oxidation reaction can be considered in dehydrogenation of methanol and water, and the formation of a second C-O bond in the Pt metal has been proposed by Oliveira<sup>19</sup>. Furthermore, Galal et al.<sup>17</sup> also demonstrated that platinum is the catalyst component that is most active in the adsorption of oxygenated species, which leads to the surface poisoning of the catalyst by the adsorbed CO (Pt(CO)<sub>ads</sub>) that blocks the catalyst surface and thereby severely limits oxidation kinetics. Consequently, the catalytic activity of the complex Pt-CMMs electrocatalyst system in the oxidation of methanol is considered to involve several steps of dehydrogenation that lead to the formation of CO<sub>ads</sub> and the oxidation reaction from CO<sub>ads</sub> to CO<sub>2</sub>, and this promotes the functional mechanism of the catalyst. Methanol is commonly considered to be adsorbed onto the surface of the catalyst before undergoing catalytic reaction at the platinum-oxide active sites. Methanol and oxygen were adsorbed onto specific sites on the complex Pt-CMMs electrocatalyst, and this promoted the rapid conversion of methanol to hydrogen and water. Furthermore, the complex Pt-CMMs electrocatalyst might have played a key role in the catalytic oxidation of methanol, whereas the CMM might have provided the active sites required for the catalyzed oxidation reaction. Conversely, the catalytic activity might also have resulted from

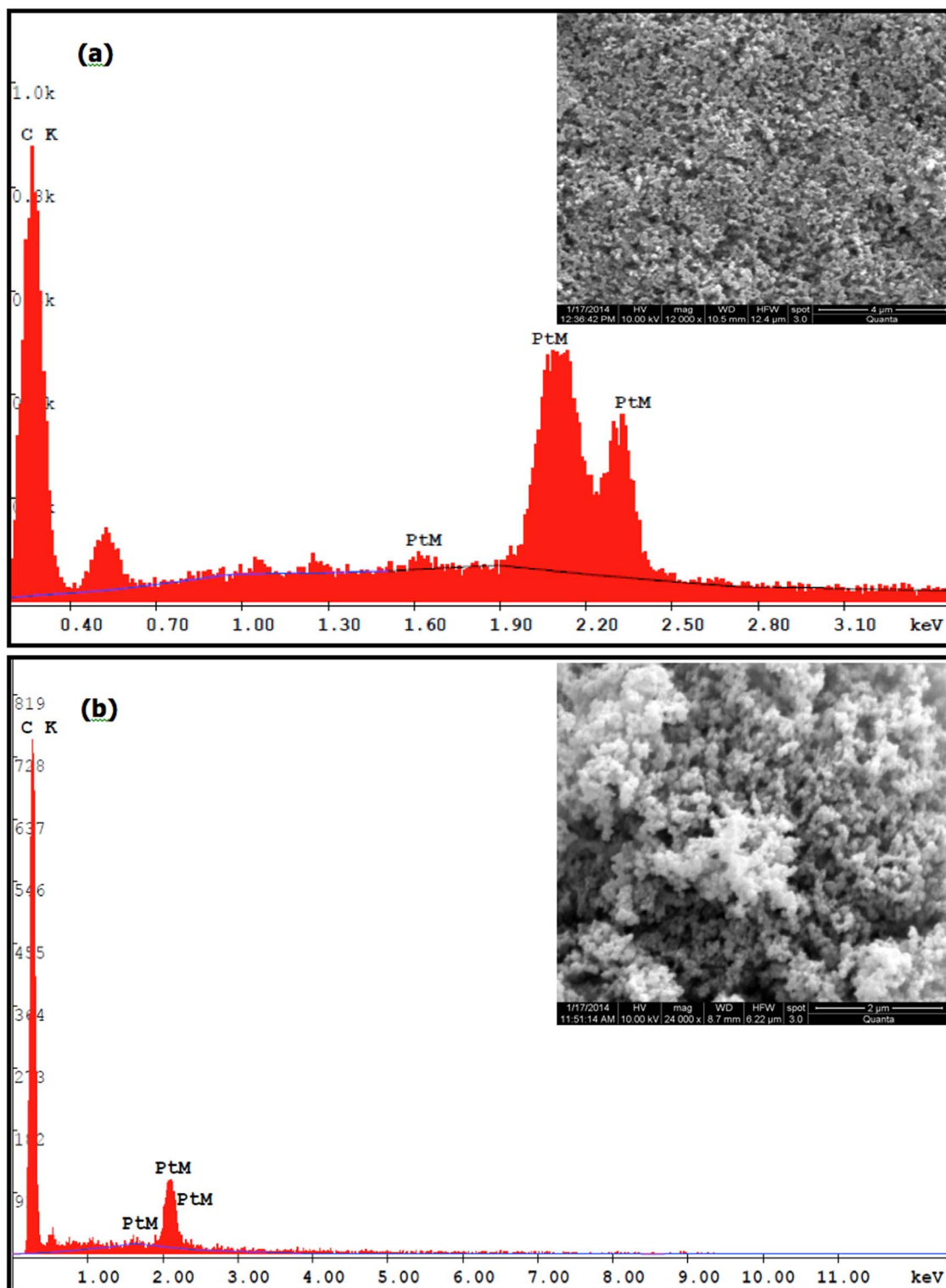


**Figure 10** | ESEM-EDS images of the Pt-CMMs electrocatalyst in a 0.5 M H<sub>2</sub>SO<sub>4</sub> + 0.1 M CH<sub>3</sub>OH solution (a) before and (b) after the electrocatalytic test.

strong interaction between the complex Pt and the CMMs. In potential scans performed at slow sweep rates of 5 and 10 mV/s, the complex Pt-CMMs electrocatalyst generated smaller methanol-oxidation peak currents in a given potential window than it did at high sweep rates (Fig. 3). This result suggests that the MOR is slowed because of the intermediate CO<sub>ads</sub> poisoning effect, which might block the adsorption and dehydrogenation of methanol on the electrocatalytic-material surface<sup>4</sup>. Moreover, when the potential scan

rate was increased, the peak potential obtained for the electrocatalysis of methanol shifted to a more positive potential, which suggested a kinetic limitation in the reaction between the redox sites of Pt-CMMs and methanol. Therefore, oxygen reduction was diffusion-controlled at potentials below 0.4 V and was under mixed diffusion-kinetic control in the potential region between 0.4 and 0.6 V as reported elsewhere<sup>38</sup>. Conversely, the oxidation of methanol might also proceed through a mechanism other than the Langmuir-



Hinshelwood mechanism, and in a previous study, Chen<sup>23</sup> proposed the Eley–Rideal mechanism for explaining the roles of the OH groups on the surface of the Ni support and of the OH<sup>-</sup> ions in the electrolyte, respectively, in the enhancement of the CO tolerance. Thus, the reaction mechanism must be investigated further to elucidate the performance of the complex Pt-CMMs electrocatalyst at the scan rates of 5 and 10 mV/s. The Pt-CMMs electrocatalyst exhibited electrocatalytic ORR activity (Fig. 4), and it also exhibited a plateau and a sharp transition of control from kinetics to diffusion, which implies a one-step, four-electron pathways of the ORR occurring on the electrodes<sup>39</sup>. Furthermore, the potential peak at 0.42 V obtained during the forward scan can be attributed to the catalytic activity during methanol oxidation; this activity might also have been resulted from the strong interaction between the complex Pt and the CMMs.

The oxidation capacity of the catalyst might account for its high methanol-electrooxidation activity, which results from the formation of Pt-OH<sub>ads</sub> at high potentials<sup>40</sup> (Fig. 5). Thus, we determined that the complex Pt-CMMs electrocatalyst plays a dominant role in the process of methanol electrocatalysis. Previously<sup>41,42</sup>, methanol was reported to be adsorbed onto the catalyst surface before undergoing an oxidation–reduction reaction at the active sites located at the electrode-electrolyte interface. The activity of the Pt-CMMs electrocatalyst decayed over time (Fig. 6), which might have occurred because of the adsorption of the intermediate products of methanol oxidation (such as CO) on the Pt-particles surface, the thermodynamic sink in the reaction, and this would have inhibited the electrooxidation reaction of methanol<sup>43</sup>.

The results of our study suggested that the catalytic activity exhibited by the complex Pt-CMMs electrocatalyst system during methanol oxidation can be explained by the catalytic behavior of the Pt and the carbon-substrate pairs, which transport protons transport highly efficiently (Fig. 7). Thus, this experimental result is similar to that obtained by Liu et al.<sup>44</sup>, who investigated methanol-decomposition reactions. Furthermore, the excitation/emission plots of the catalyst can be described based on the metal-enhanced fluorescence effect (Fig. 8), in which fluorescence is associated with the Pt clusters that are present on the surface of the complex Pt-CMMs electrocatalyst during the reaction<sup>45</sup>. When oxidation occurred over the Pt-CMMs catalyst, the platinum was transformed from the oxide form to the metal form (Fig. 9). The platinum in a CMM can be assumed to promote the formation of the active phase of PtO<sub>2</sub> upon the oxidation of methanol. The results of XRD experiments indicated that platinum (IV) oxide active sites were formed on the Pt-CMMs catalyst. Therefore, methanol can be considered to have been adsorbed on the surface of the catalyst before undergoing an electrocatalytic reaction at the platinum-oxide active sites. The high dispersion and uniform distribution of the Pt catalyst within the carbon support can enhance the electrocatalytic activity of the Pt-CMMs catalyst. Moreover, the results shown in Fig. 10 indicates that platinum and carbon can leach from the catalyst, which reduces the surface activity of platinum. Elemental-composition analysis of the test catalysts' surfaces revealed that the leaching of metal ions from the Pt-CMMs catalyst varied slightly. Platinum eluted from the catalyst, which likely rendered the active site of the carbon an exposed surface. In the case of carbon-supported catalysts, performance is lost mainly because of carbon corrosion, which leads to the agglomeration of Pt particles on the surface of the support<sup>46</sup>. Furthermore, the ESEM results showed that the aged Pt particles were highly dispersed on the CMM and featured a diameter of approximately ~40 nm and a narrow particle-size distribution.

## Methods

**Materials.** The Pt-CMM substrate catalyst that was used in this study was prepared through the process of incipient wetness impregnation, which involved using aqueous H<sub>2</sub>PtCl<sub>6</sub>. Before depositing, the carbon mesoporous substrate was first refluxed in a nitrate-acid solution, and this treated carbon substrate was then filtered and washed with deionized water and dried at 333 K in an oven for 6 h. Subsequently, the

platinum catalyst was coated on a high-surface-area CMMs (Vulcan XC-72 carbon black) and the platinum active metal was maintained at 10 wt%. After the coating process, the mixture was ultrasonically homogenized for 30 min and stirred for 2 h, and the resulting powders formed were fashioned into tablets by using acetic acid as a binder. The tablets were later reheated at 573 K and the catalyst was calcined at 673 K in an air stream for 6 h to burn out the binder used in tablets. The tablets were then crushed and sieved to obtain particles ranging in size from 0.25 to 0.15 mm, which were used in various experiments.

**Analyses.** To investigate the electrochemical behavior of the electrode samples, LSV, polarization-curve and chronoamperometric measurements were obtained at room temperature by using an electrochemical analyzer (CHI 6081D, USA) that was equipped with a 3D electrochemical cell. The ORR was evaluated based on LSV measurements obtained using a rotating disk electrode (RDE) technique. The working electrode (WE) was a glassy carbon electrode, and in each analysis, the samples were scanned at rates of 5, 10, 50 and 100 mV/s and the potential was cycled between -0.2 and 1.2 V. The counter electrode (CE) was a platinum wire, and a saturated hydrogen electrode (SHE) was used as the reference electrode (RE). The H<sub>2</sub>SO<sub>4</sub> (0.5 M) electrolyte was saturated with high-purity oxygen for at least 30 min. The ORR polarization curves were obtained in the potential range of 0.1 to 1.0 V by using scanning rates of 5, 10, 50 and 100 mV/s and a rotating speed of 1600 rpm at room temperature. In this study, the catalyst ink was prepared using the following procedure: First, 5 mg of the Pt-particle carbon mesoporous substrate catalyst was added to 2.5 mL of deionized water and ultrasonicated for 30 min. Subsequently, approximately 20 μL of the resulting mixture was withdrawn and deposited onto a polished-glass carbon electrode and allowed to dry in air at 333 K for 60 min. Finally, 20 μL of 5% Nafion solution was added as a binder onto the disk in a nitrogen environment<sup>12,15</sup>. FEEM spectroscopy was performed to fully characterize the spectra of the catalyst material; the EEFM spectra were obtained using a luminescence spectrophotometer (F-4500, Hitachi, Japan) equipped with a xenon lamp as the excitation source. The emission spectra were plotted along the x-axis and the excitation spectra were plotted along the y-axis. All slit widths in the excitation and the emission monochromators were 10 nm. The EEFMs obtained comprised 60 excitation and 60 emission spectra in the 200–800 nm range, and this yielded discrete values of the fluorescence intensities at 3600 excitation/emission wavelength pairs; from these spectra, blank spectra of pure water were subtracted. The UV-Vis absorption spectra of the solid sample were obtained using a photo spectrophotometer (U-2900, Hitachi, Japan). XRD analysis was performed using a Diano-8536 diffractometer equipped with a CuKα radiation source. During analyses, samples were scanned from 10° to 80° at a rate of 0.4°/min. We used an ESEM system equipped with an EDS (Quanta 200 FEG, FEI Company, Czech Republic) to elucidate the morphology of the catalyst; these studies yielded information on the distribution of the Pt-CMMs composite present on the catalyst surface.

- Kashyout, A. B., Nassr, A. B. A. A., Giorgi, L., Maiyalagan, T. & Youssef, B. A. B. Electrooxidation of methanol on carbon supported Pt-Ru nanocatalysts prepared by ethanol reduction method. *Int. J. Electrochem. Sci.* **6**, 379–393 (2011).
- Jiang, X., Gür, T. M., Prinz, F. B. & Bent, S. F. Atomic layer deposition (ALD) co-deposited Pt-Ru binary and Pt skin catalysts for concentrated methanol oxidation. *Chem. Mater.* **22**, 3024–3032 (2010).
- Routray, K., Zhou, W., Kiely, C. J. & Wachs, I. E. Catalysis science of methanol oxidation over iron vanadate catalysts: Nature of the catalytic active sites. *Catal.* **1**, 54–66 (2011).
- Sun, J., Huang, J., Cao, Y. & Zhang, X. Hydrothermal synthesis of Pt-Ru/MWCNTs and its electrocatalytic properties for oxidation of methanol. *Int. J. Electrochem. Sci.* **2**, 64–71 (2007).
- Chen, J. et al. Studies on how to obtain the best catalytic activity of Pt/C catalyst by three reduction routes for methanol electro-oxidation. *Chem. Commun.* **13**, 314–316 (2011).
- Chen, C. S. & Pan, F. M. Electrocatalytic activity of Pt nanoparticles deposited on porous TiO<sub>2</sub> supports toward methanol oxidation. *Applied Catal. B: Environ.* **91**, 663–669 (2009).
- Hsu, N. Y., Chien, C. C. & Jeng, K. T. Characterization and enhancement of carbon nanotube-supported PtRu electrocatalyst for direct methanol fuel cell applications. *Applied Catal. B: Environ.* **84**, 196–203 (2008).
- Karim-Nezhad, G. & Dorraji, P. S. Copper chloride modified copper electrode: Application to electrocatalytic oxidation of methanol. *Electrochimica Acta* **55**, 3414–3420 (2010).
- Lo, A. Y. et al. Fabrication of CNTs with controlled diameters and their applications as electrocatalyst supports for DMFC. *Diamond Related Mat.* **20**, 343–350 (2011).
- Tang, Z. & Lu, G. Synthesis and characterization of high performance Pt-(Pr<sub>x</sub>CeyO<sub>2</sub>)/C catalysts for methanol electrooxidation. *Applied Catal. B: Environ.* **79**, 1–7 (2008).
- Feng, X. J., Shi, Y. L. & Hu, Z. A. PAN/PSF composite films as supports of PtRu particles for methanol electro-oxidation. *Int. J. Electrochem. Sci.* **5**, 489–500 (2010).
- Liu, S. H., Zheng, F. S. & Wu, J. R. Preparation of ordered mesoporous carbons containing well-dispersed and highly alloying Pt-Co bimetallic nanoparticles toward methanol-resistant oxygen reduction reaction. *Applied Catal. B: Environ.* **108–109**, 81–89 (2011).



13. Nikonova, O. A. *et al.* Novel approach to rhenium oxide catalysts for selective oxidation of methanol to DMM. *J. Catal.* **279**, 310–18 (2011).
14. Huang, Y. J., Ng, K. L. & Huang, H. Y. The effect of gold on the copper-zinc oxides catalyst during the partial oxidation of methanol reaction. *Int. J. Hydrogen Energy* **36**, 15203–15211 (2011).
15. Liu, S. H. *et al.* Fabrication and characterization of well-dispersed and highly stable PtRu nanoparticles on carbon mesoporous material for applications in direct methanol fuel cell. *Chem. Mater.* **20**, 1622–1628 (2008).
16. Lee, J. M. *et al.* Methanol electrooxidation of Pt catalyst on titanium nitride nanostructured support. *Applied Catal. A: Gen.* **375**, 149–155 (2010).
17. Galal, A., Atta, N. F. & Hassan, H. K. Graphene supported-Pt-M (M = Ru or Pd) for electrocatalytic methanol oxidation. *Int. J. Electrochem. Sci.* **7**, 68–84 (2012).
18. Xie, S. W., Chen, S., Liu, Z. Q. & Xu, C. W. Comparison of alcohol electrooxidation on Pt and Pd electrodes in alkaline medium. *Int. J. Electrochem. Sci.* **6**, 882–8 (2011).
19. Oliveira, R. T. S. *et al.* Nanogravimetric and voltammetric studies of a Pt-Rh alloy surface and its behavior for methanol oxidation. *Int. J. Electrochem. Sci.* **3**, 970–979 (2008).
20. Ren, F. *et al.* Fabrication of poly(*o*-methoxyaniline)/Pt-M nanocomposites and their electrocatalytic activities for methanol oxidation. *Int. J. Electrochem. Sci.* **6**, 5701–5709 (2011).
21. Du, H. Y. *et al.* Controlled platinum nanoparticles uniformly dispersed on nitrogen-doped carbon nanotubes for methanol oxidation. *Diamond Related Mat.* **17**, 535–41 (2008).
22. Gregoire, J. M. *et al.* Improved fuel cell oxidation catalysis in Pt<sub>1-x</sub>Ta<sub>x</sub>. *Chem. Mater.* **22**, 1080–1087 (2010).
23. Chen, C. S., Pan, F. M. & Yu, H. J. Electrocatalytic activity of Pt nanoparticles on a karst-like Ni thin film toward methanol oxidation in alkaline solutions. *Applied Catal. B: Environ.* **104**, 382–389 (2011).
24. Salgado, J. R. C. *et al.* Effect of functionalized carbon as Pt electrocatalyst support on the methanol oxidation reaction. *Applied Catal. B: Environ.* **102**, 496–504 (2011).
25. Song, S. *et al.* The effect of microwave operation parameters on the electrochemical performance of Pt/C catalysts. *Applied Catal. B: Environ.* **103**, 3287–3293 (2011).
26. Antolini, E. Platinum-based ternary catalysts for low temperature fuel cells Part I. Preparation methods and structural characteristics. *Applied Catal. B: Environ.* **74**, 324–336 (2007).
27. Antolini, E. Platinum-based ternary catalysts for low temperature fuel cells Part II. Spectrochemical properties. *Applied Catal. B: Environ.* **74**, 337–350 (2007).
28. Herrera-Méndez, H. D. *et al.* Carbon-supported platinum molybdenum electrocatalysts and their electro-activity toward ethanol oxidation. *Int. J. Electrochem. Sci.* **6**, 4454–4469 (2011).
29. Raouf, J. B., Jahanshahi, M. & Ahangar, S. M. Nickel particles dispersed into poly(*o*-anisidine) and poly(*o*-anisidine)/mutile-walled carbon nanotube modified glassy carbon electrodes for electrocatalytic oxidation of methanol. *Inter. J. Electrochem. Sci.* **5**, 517–530 (2010).
30. Wu, M. L. & Lai, L. B. Synthesis of Pt/Ag bimetallic nanoparticles in water-in-oil microemulsions. *Colloids and Surfaces A: Physico. Eng. Aspects.* **244**, 149–157 (2004).
31. Hirakawa, K., Inoue, M. & Abe, T. Methanol oxidation on carbon-supported Pt–Ru and TiO<sub>2</sub> (Pt–Ru/TiO<sub>2</sub>/C) electrocatalyst prepared using polygonal barrel-sputtering method. *Electrochem. Acta.* **55**, 5874–5880 (2010).
32. Pérez-Ramírez, J. *et al.* Characterization and performance of Pt-USY in the SCR of NO<sub>x</sub> with hydrocarbons under lean-burn conditions. *Applied Catal. B: Environ.* **29**, 285–298 (2001).
33. Shin, H. K., Hirahayashi, H., Yahiro, H., Watanabe, M. & Iwamoto, M. Selective catalytic reduction of NO by ethene in excess oxygen over platinum ion-exchanged MFI zeolites. *Catal. Today* **26**, 13–21 (1995).
34. Chen, J. *et al.* Mesoporous carbon spheres: Synthesis, characterization and supercapacitance. *Int. J. Electrochem. Sci.* **4**, 1063–1073 (2009).
35. Yao, K. & Cheng, Y. F. Electrodeposited Ni–Pt binary alloys as electrocatalysts for oxidation of ammonia. *J. Power Sources.* **173**, 96–101 (2007).
36. Lin, R. B. & Shih, S. M. Cyclic voltammetric measurement of catalyst surface area for Pt-black/naftion electrodes. *J. Chin. Inst. Chem. Engrs.* **37**, 311–319 (2006).
37. Oliveira, R. T. S., Santos, M. C., Nascence, P. A. P., Bulhões, L. O. S. & Pereira, E. C. Nanogravimetric and voltammetric studies of a Pt-Rh alloy surface and its behavior for methanol oxidation. *Inter. J. Electrochem. Sci.* **3**, 970–979 (2008).
38. Narayanamoorthy, B., Datta, K. K. R. & Balaji, S. Kinetics and mechanism of electrochemical oxygen reduction using platinum/clay/Nafion catalyst layer for polymer electrolyte member fuel cells. *J. Colloid and Interface Sci.* **387**, 213–220 (2012).
39. Wang, R. *et al.* Nitrogen-rich mesoporous carbon derived from melamine with high electrocatalytic performance for oxygen reduction reaction. *J. Power Sources* **261**, 238–244 (2014).
40. Yoo, S. J., Jeon, T. Y., Cho, Y. H., Lee, K. S. & Sung, Y. E. Particle size effects of PtRu nanoparticles embedded in TiO<sub>2</sub> on methanol electrooxidation. *Electrochem. Acta.* **55**, 7939–7944 (2010).
41. Wang, S., Jiang, S. P., Wang, X. & Guo, J. Enhanced electrochemical activity of Pt nanowire network electrocatalysts for methanol oxidation reaction of fuel cells. *Electrochem. Acta.* **56**, 1563–1569 (2011).
42. Scibioh, M. A., Oh, I. H., Lim, T. H., Hong, S. A. & Ha, H. Y. Investigation of various ionomer-coated carbon supports for direct methanol fuel cell applications. *Applied Catal. B: Environ.* **77**, 373–385 (2008).
43. Huang, H. X., Chen, S. X. & Yuan, C. Platinum nanoparticles supported on activated carbon fiber as catalyst for methanol oxidation. *J. Power Sources.* **175**, 166–174 (2008).
44. Liu, Y., Zheng, N., Chao, W., Liu, H. & Wang, Y. A novel nanocomposite catalytic cathode for direct methanol fuel cells. *Electrochem. Acta.* **55**, 5617–5623 (2010).
45. Zhang, S. & Zhao, Y. Facile preparation of organic nanoparticles by interfacial cross-linking of reversed micelles and template synthesis of subnanometer Au-Pt nanoparticles. *Nano.* **5**, 2637–2646 (2011).
46. Kumar, R., Pasupathi, S., Pollet, B. G. & Ccort, K. Nafion-stabilised platinum nanoparticles supported on titanium nitride: An efficient and durable electrocatalyst for phosphoric acid based polymer electrolyte fuel cells. *Electrochimica Acta* **109**, 365–369 (2013).

## Acknowledgments

The author would like to thank the National Science Council of the Republic of China, Taiwan, for financial support of this research under Contract No. NSC 101-2221-E-132-001. The author also thanks Prof. Wen-Liang Lai from the Department of Environmental Science and Occupational Safety and Hygiene at Tajen University of Science and Technology for his support and discussions.

## Author contributions

Cheng-Di, Chiu-Wen and Chih-Feng discussed the results in detail. Chang-Mao designed the study and wrote the main manuscript text and prepared figures. All authors reviewed the manuscript.

## Additional information

This paper was presented at the Asia-Pacific Conference on Electrochemical Energy Storage and Conversion (APEnergy2014), Brisbane, Australia, February 5–8.

**Competing financial interests:** The authors declare no competing financial interests.

**How to cite this article:** Dong, C.-D., Chen, C.-W., Chen, C.-F. & Hung, C.-M. Platinum particles supported on mesoporous carbons: fabrication and electrocatalytic performance in methanol-tolerant oxygen-reduction reactions. *Sci. Rep.* **4**, 5790; DOI:10.1038/srep05790 (2014).



This work is licensed under a Creative Commons Attribution-NonCommercial-NoDerivs 4.0 International License. The images or other third party material in this article are included in the article's Creative Commons license, unless indicated otherwise in the credit line; if the material is not included under the Creative Commons license, users will need to obtain permission from the license holder in order to reproduce the material. To view a copy of this license, visit <http://creativecommons.org/licenses/by-nc-nd/4.0/>